A heterometallic Zn-Eu MOF as a sensor with the identification of folic acid and sulfaquinoxaline

Dechao Li,Yuejiao Jia,Zhang Li, Lu Liu, Nan Wu, Ming Hu

Inner Mongolia Key Laboratory of Chemistry and Physics of Rare Earth Materials; School of Chemistry and Chemical Engineering, Inner Mongolia University, Hohhot 010021, China. Tel.: +86-471-4992981. E-mail addresses: hm988@126.com.

1. EXPERIMENTAL SECTION

1.1 Materials and general methods

All chemicals were commercially purchased and used without further purification. The IR spectra were recorded as KBr pellets on a Nicolet Avatar-360 spectrometer in the 400-4000 cm^{-1} region. The thermogravimetric analyses (TGA) were conducted on a PerkinElmer TG-7 analyzer heated from 30 to 1400℃ under a nitrogen atmosphere. The powder X-ray diffraction (PXRD) measurements were performed on an Analytical Empyrean instrument using Cu-*Kα* radiation at room temperature. The luminescence spectra were measured on a FLS920 spectrophotometer. The UV-vis spectroscopic studies were recorded on a Hitachi U-3900 spectrophotometer. The X-ray photoelectron spectroscopy (XPS) was obtained on a Thermo Scientific ESCALAB 250Xi photoelectron spectrometer.

1.2 X-Ray crystallography

Crystallographic data for **1** were collected on a Bruker Smart 1000 diffractometer equipped with graphite-monochromatic Mo-*Kα* radiation (λ = 0.71073 Å) using the ω-scan technique at room temperature. Semiempirical absorption corrections were applied using the SADABS program. The structure was solved by direct methods using SHELXS-2018 and was refined by full matrix leastsquares on $|F|^2$ using the SHELXTL-2018 program. All non-hydrogen atoms were refined anisotropically. The organic hydrogen atoms were geometrically generated, the hydrogen atoms of water molecules were located from difference Fourier maps and refined with the common isotropic thermal parameter. Details of the crystal parameter data collection and refinement for **1** are summarized in Table S1. The selected bond lengths and angles of **1** are listed in Table S2, and the CCDC No. for **1** is 2167746.

2. SUPPLEMENTARY FIGURES AND TABLES

Table S1. The crystal data for **1**

Complex	**1**
Formula	$C_{25}H_{23}EuN_4O_{15}Zn$
Formula weight	836.80
T/K	100.01(10)
Crystal system	monoclinic
Space group	*C*2/*c*
a(Å)	24.5485(3)
b(Å)	12.59520(10)
c(Å)	18.3397(2)
α(°)	90
β (°)	104.2490(10)
γ(°)	90
V(Å^3)	5496.06(10)
Z	8
D_{calc}(g cm^{-3})	2.023
μ (mm^{-1})	18.021
F(000)	3312.0
Rint	0.0220
GOOF	1.039
R_1[a] [I > 2σ(I)]	0.0212
ωR_2[b] [I > 2σ(I)]	0.0563
R_1 (all data)	0.0224
wR_2 (all data)	0.0569
largest diff. peak and hole (e Å^{-3})	0.45，-1.10
[a]$R_1=\Sigma\|\|F_o\|-\|F_c\|\|/\Sigma\|F_o\|$. [b]$\omega R_2=[\Sigma[\omega(F_o^2-F_c^2)^2]/\Sigma\omega(F_o^2)^2]^{1/2}$.	

Table S2. Selected bond lengths [Å] and angles [°] for **1**

Complex 1			
Eu(1)-O(14)	2.3802(15)	Eu(1)-O(4)	2.4779(13)
Eu(1)-O(7)	2.7051(13)	Eu(1)-O(5)	2.5203(13)
Eu(1)-O(8)	2.4678(13)	Eu(1)-O(1)	2.3403(13)
Eu(1)-O(13)	2.4363(13)	Eu(1)-O(3)	2.5157(14)
Eu(1)-O(6)	2.4826(13)	Zn(1)-O(10)	2.1116(14)
Zn(1)-O(9)	2.1061(14)	Zn(1)-N(3)	2.1860(16)
Zn(1)-N(4)	2.1165(15)	Zn(1)-N(2)	2.1058(16)
Zn(1)-N(1)	2.1674(16)		
O(14)-Eu(1)-O(4)	86.83(5)	O(14)-Eu(1)-O(7)	74.80(5)
O(14)-Eu(1)-O(5)	143.66(5)	O(14)-Eu(1)-O(8)	122.35(5)
O(14)-Eu(1)-O(13)	76.82(5)	O(14)-Eu(1)-O(3)	88.77(5)
O(14)-Eu(1)-O(6)	159.61(5)	O(4)-Eu(1)-O(7)	118.75(4)
O(4)-Eu(1)-O(5)	114.01(4)	O(4)-Eu(1)-O(3)	52.46(4)
O(4)-Eu(1)-O(6)	72.88(4)	O(5)-Eu(1)-O(7)	114.76(4)
O(8)-Eu(1)-O(4)	130.36(5)	O(8)-Eu(1)-O(7)	50.00(4)
O(8)-Eu(1)-O(5)	67.27(4)	O(8)-Eu(1)-O(3)	86.14(5)
O(8)-Eu(1)-O(6)	72.12(5)	O(1)-Eu(1)-O(14)	82.11(5)
O(1)-Eu(1)-O(4)	71.36(4)	O(1)-Eu(1)-O(7)	153.77(4)
O(1)-Eu(1)-O(5)	77.51(5)	O(1)-Eu(1)-O(8)	143.84(5)
O(1)-Eu(1)-O(13)	77.27(5)	O(1)-Eu(1)-O(3)	123.50(4)
O(1)-Eu(1)-O(6)	93.05(5)	O(13)-Eu(1)-O(4)	146.29(4)
O(13)-Eu(1)-O(7)	85.39(4)	O(13)-Eu(1)-O(5)	69.56(4)

O(13)-Eu(1)-O(8)	82.86(5)	O(13)-Eu(1)-O(3)	153.21(4)
O(13)-Eu(1)-O(6)	121.59(4)	O(3)-Eu(1)-O(7)	68.93(4)
O(3)-Eu(1)-O(5)	127.57(4)	O(6)-Eu(1)-O(7)	112.88(4)
O(6)-Eu(1)-O(5)	52.21(4)	O(6)-Eu(1)-O(3)	77.36(4)
O(10)-Zn(1)-N(3)	92.89(6)	O(10)-Zn(1)-N(4)	95.98(6)
O(10)-Zn(1)-N(1)	165.54(6)	O(9)-Zn(1)-O(10)	85.63(6)
O(9)-Zn(1)-N(3)	166.48(6)	O(9)-Zn(1)-N(4)	90.53(6)
O(9)-Zn(1)-N(1)	87.23(6)	N(4)-Zn(1)-N(3)	76.24(6)
N(4)-Zn(1)-N(1)	96.65(6)	N(2)-Zn(1)-O(10)	92.54(6)
N(2)-Zn(1)-O(9)	100.77(6)	N(2)-Zn(1)-N(3)	92.71(6)
N(2)-Zn(1)-N(4)	166.34(6)	N(2)-Zn(1)-N(1)	76.46(6)

Table S3. Fluorescent quantum yield data of compound **1**

Compound **1**			
ν_{00} (cm^{-1})	17241	A_{00}	5.976
ν_{01} (cm^{-1})	16891	A_{01}	50
ν_{02} (cm^{-1})	16233	A_{02}	556.434
ν_{03} (cm^{-1})	15384	A_{03}	9.477
ν_{04} (cm^{-1})	14285	A_{04}	42.468
I_{01} (a.u)	39050	**Ar**	**664.355**
I_{02} (a.u)	415700	**τ (ms)**	**0.42**
I_{02}/I_{01}	10.65	**$1/\tau$**	**2.38**
η%		**27.91**	

The luminescence quantum yield η of the $^5D_0$ emission lever in the ternary Eu(III) complex could be calculated based on the measurements: Eq. (1) is a means to determine the η values from experimental spectroscopic data,

η = Ar /(Ar +Anr) Eq. (1)

where Ar and Anr are radiative and non-radiative transition rates, respectively. The denominator in Eq. (1) is calculated from the lifetime of the emitting level ($1/\tau$ = Ar +Anr, where τ stands for fluorescence lifetime).

In the case of europium luminescence, value of Ar could be obtained from the Eq. (2),

$Ar = \Sigma A_{0J} = A_{00}+A_{01}+A_{02}+A_{03}+A_{04}$ Eq. (2)

where J represents the final $^7F_{0\text{-}4}$ levers. The values of A_{0J} could be calculated by the Eq. (3) and Eq. (4) ,

$A_{0J} = A_{01}(I_{0J}/I_{01})(\nu_{01}/\nu_{0J})$ Eq. (3)

$\nu_{0J} = 1/\lambda_J$ Eq. (4)

Where λ stands for wavelength correspondingly, A_{01} is the Einstein coefficient of spontaneous emission between the $^5D_0$ and the $^7F_1$ Stark levels, which may be used as a reference for the whole spectrum in vacuum, A_{01} = 50 s^{-11}. The needed calculated responding data are shown in Table S3.

Table S4 Comparison of various methods for detecting FA.

Materials	K_{SV} **(M^{-1})**	**Detection Limit**	**Ref.**
Carbon dots	/	40 nM	1
{Tb(BTC)DMF}$_n$ （bulk-Tb-MOFs）	$1.767 \times 10^4\ M^{-1}$	16.78 μM	2
Eu(HDPB)(phen)	$3.44 \times 10^4\ M^{-1}$	1.55×10^{-6}M	3
Fe_3O_4 NPs	/	9.6 ng/mL	4
nMOFs/Au NCs	/	45 nM	5
Eu-MOF	/	3×10^{-7}M	6
$[EuZn(LZ)_2(HCOO)(H_2O)_3]_n$	$3.94\times 10^5\ M^{-1}$	1.84×10^{-8} M	This work

Table S5 HOMO and LUMO energies calculated for ligand L and analyte at B3LYP/6-31G(d).

	LOMO (eV)	HUMO (eV)	Band Gap (eV)
L	−2.3922	−7.3520	4.9598
FA	−2.3260	−5.8121	3.4861
SQX	−1.8063	−6.0208	4.2145

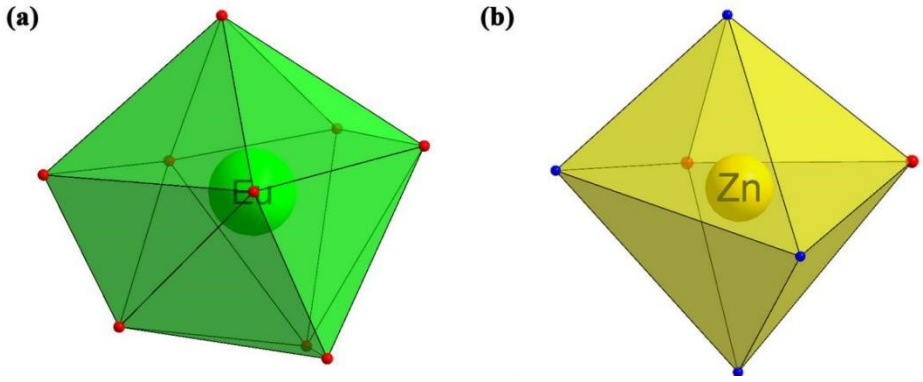

Figure S1. (a) The distorted monocapped square antiprism polyhedron of Eu^{3+} ion; (b)The twisted octahedron polyhedron of Zn^{2+} ion.

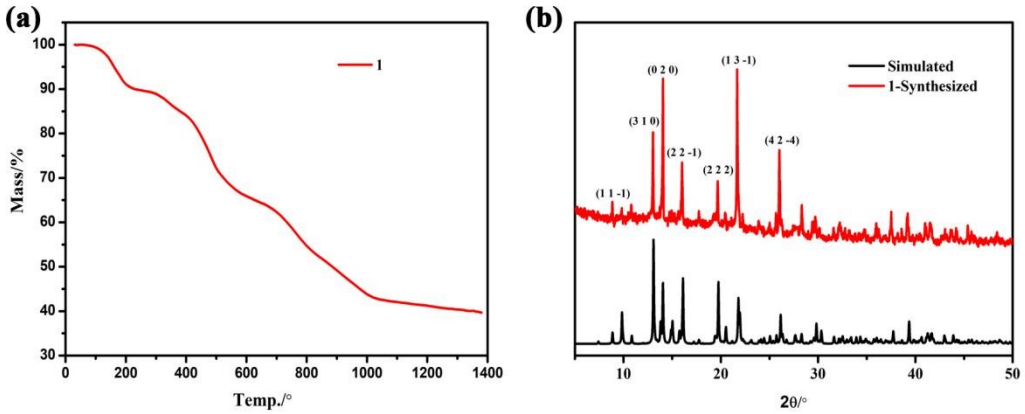

Figure S2. (a) The TGA curve of **1**; (b) The simulated PXRD pattern and experimental PXRD one of **1**.

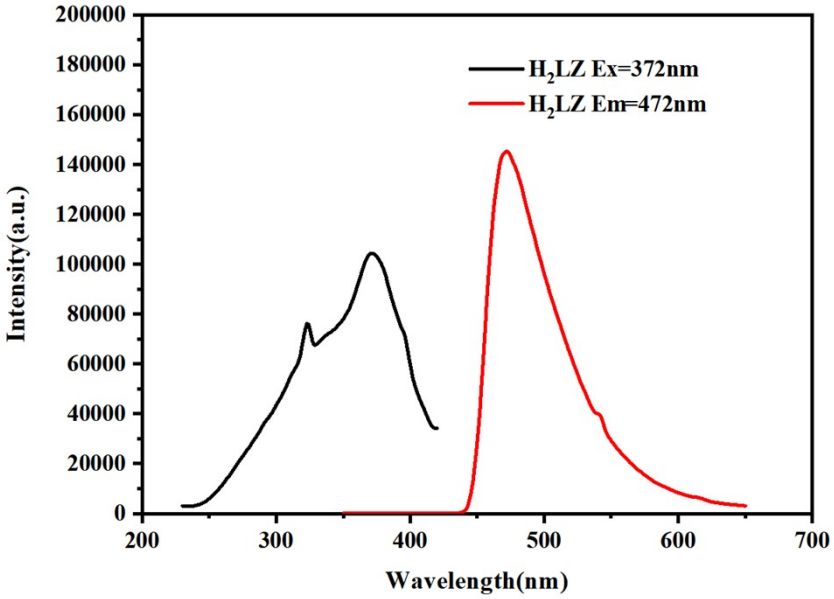

Figure S3. The PL spectra of H_2LZ.

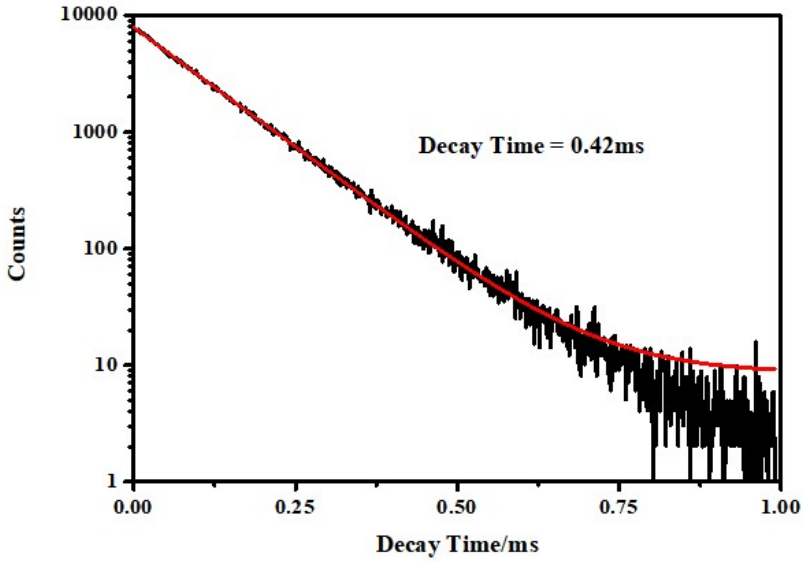

Figure S4. The fluorescence decay and fit curve for MOF **1**.

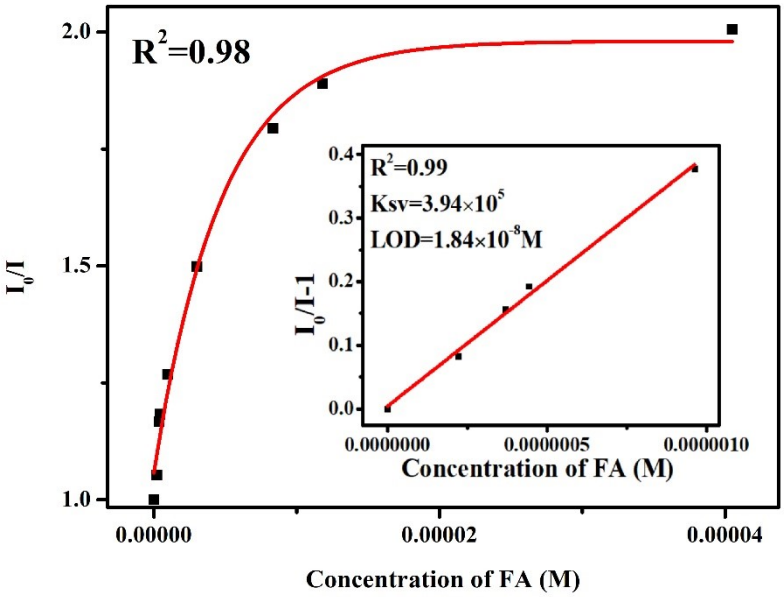

Figure S5. The linear relationship between quenching intensity and FA concentration.

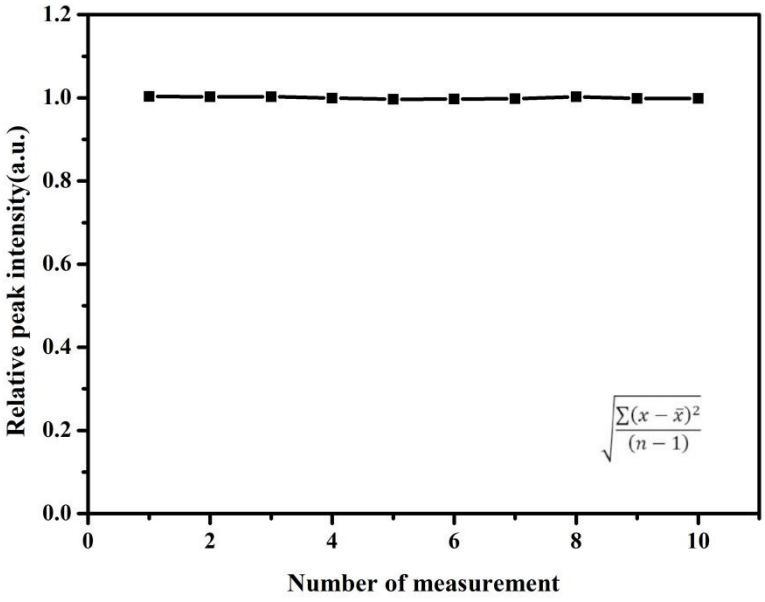

Figure S6. Calibration curve with blank measurements after ten cycles (insert: thestandard deviation formula, where x, $\bar{x}$ and n represent the luminescence intensity values of MOF **1** after normalization, the average of the maximum luminescence intensity values of MOF **1** after ten cycles and the cycles of blank measurements, respectively). Calculated standard deviation, σ = 0.002415.

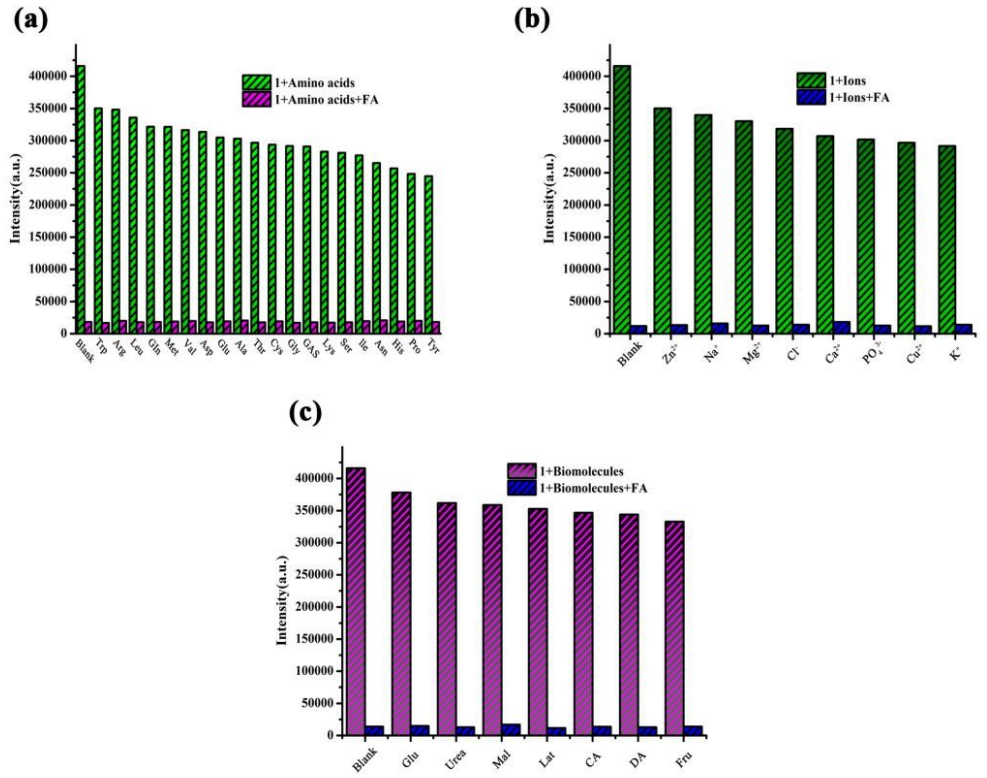

Figure S7. Competitive experiments in the absence and presence of (a) Biological amino acids; (b) Biological ions; (c) Common biological molecules.

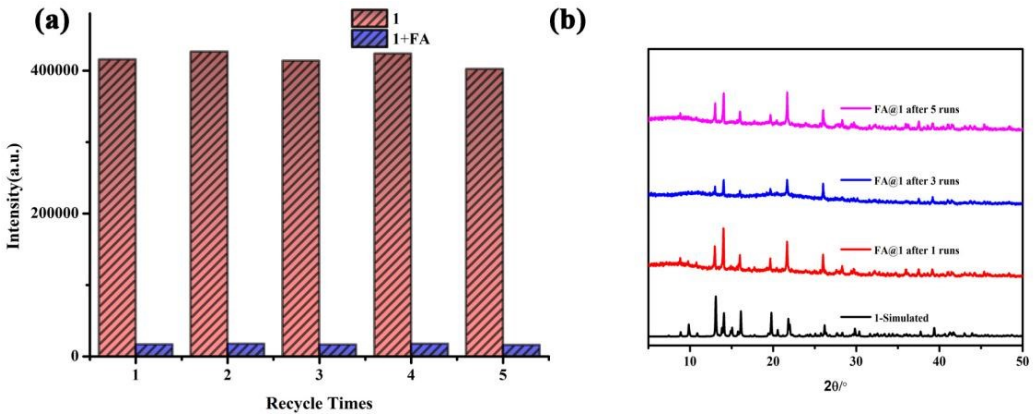

Figure S8. (a) Recyclability of complex **1** immerses in FA; (b) PXRD patterns of complex **1** after sensing five times.

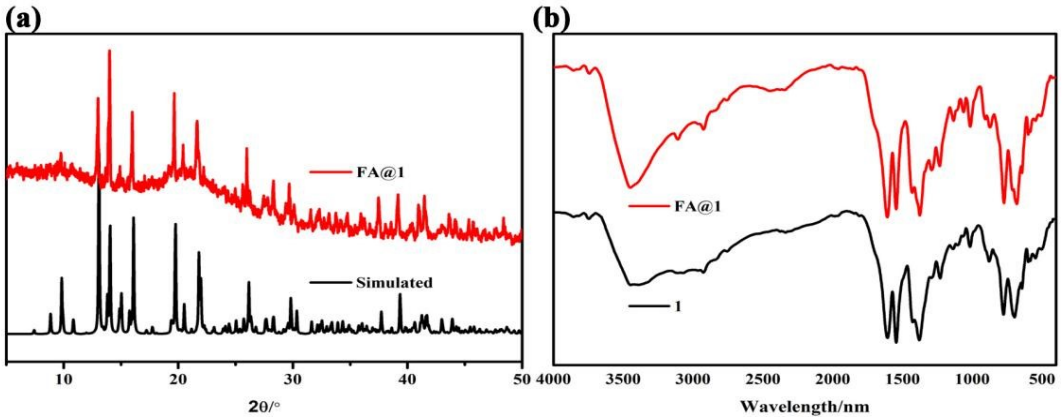

Figure S9. (a) Effect of FA on PXRD pattern of complex **1**; (b) The IR spectra of **1**, **1** soaked in FA aqueous solutions.

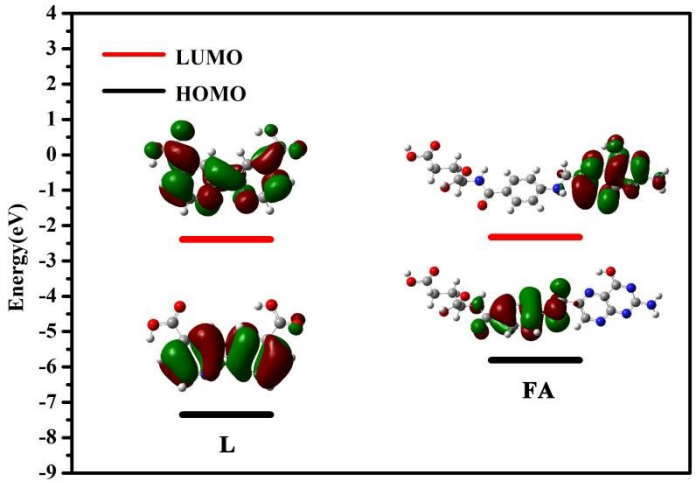

Figure S10. The HOMO and LUMO energies for FA and L [B3LYP/6-31G(d)].

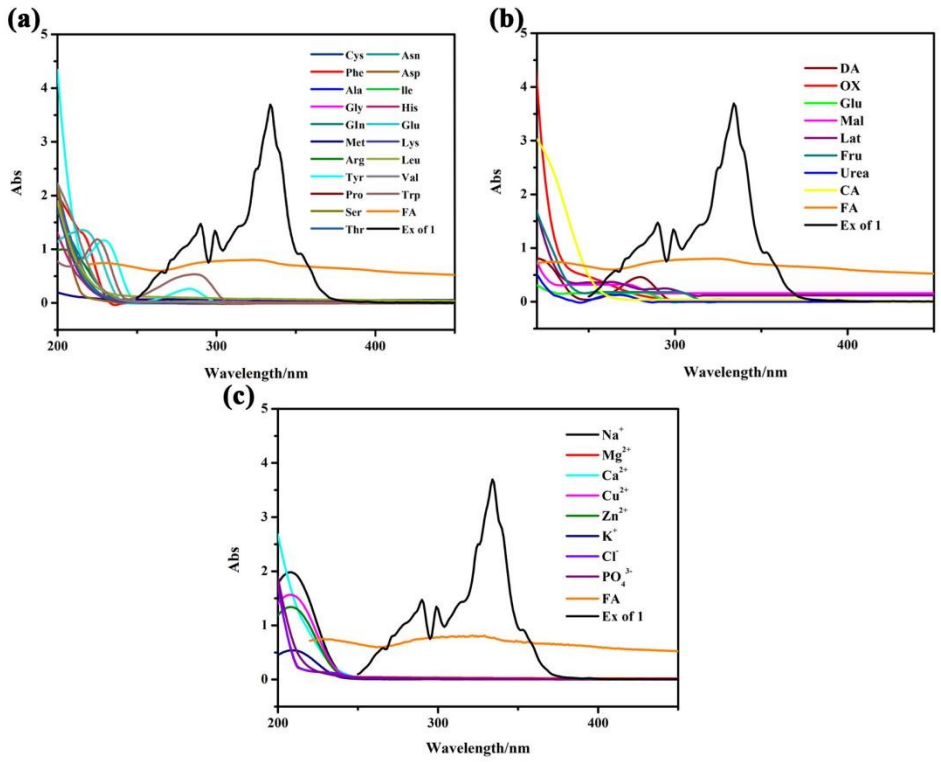

Figure S11. UV-vis absorption spectrum of (a) Biological amino acids; (b) Common biological molecules; (c) Biological ions and the excitation spectrum of complex **1**.

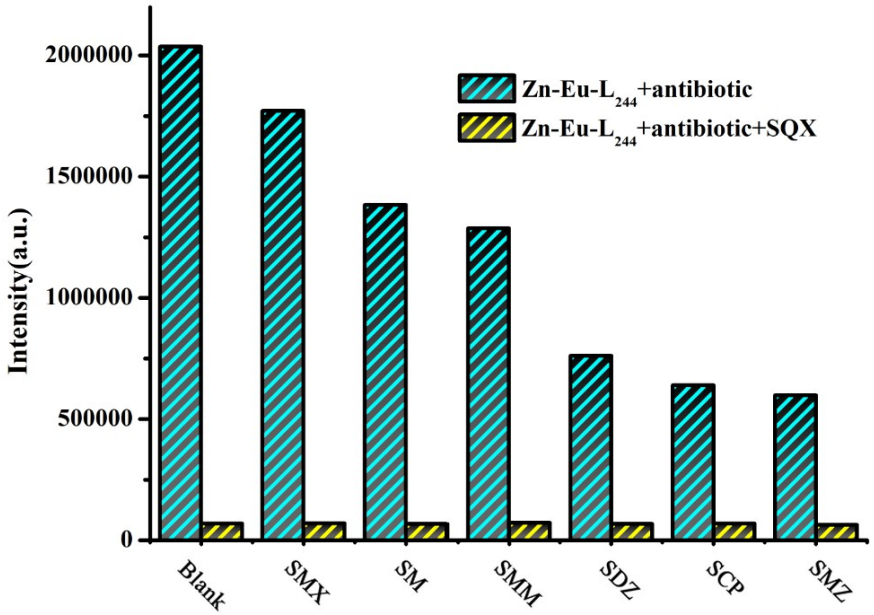

Figure S12. Comparison of fluorescence intensity of **1** at 616nm after different sulfadiazine antibiotics and addition of SQX.

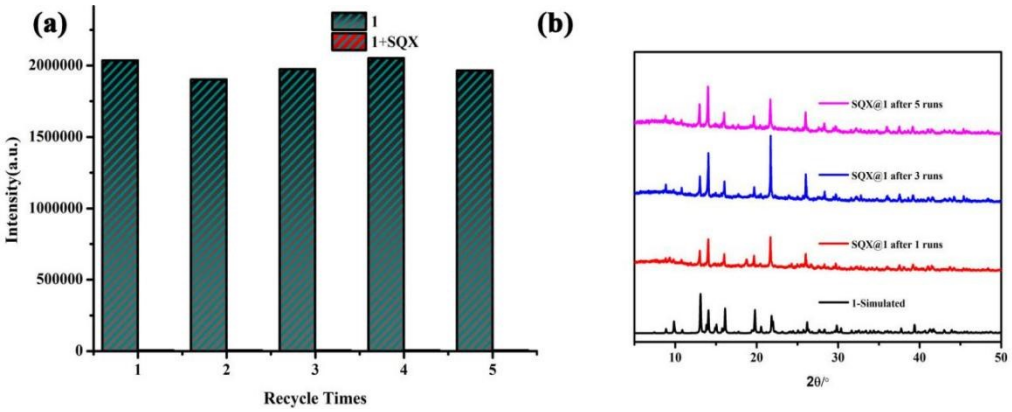

Figure S13. (a) Recyclability of complex **1** immerses in DMF with SQX; (b) PXRD patterns of complex **1** after sensing five times.

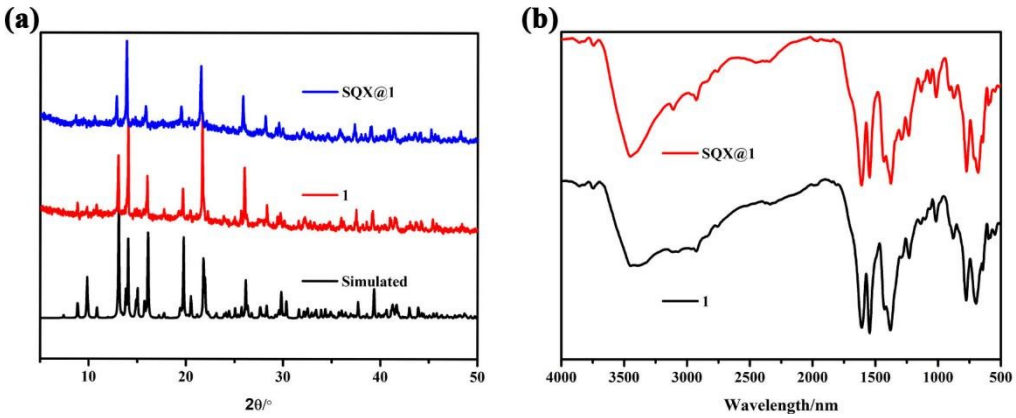

Figure S14. (a) Effect of SQX on PXRD pattern of complex **1**; (b) The IR spectra of **1** and SQX@**1**.

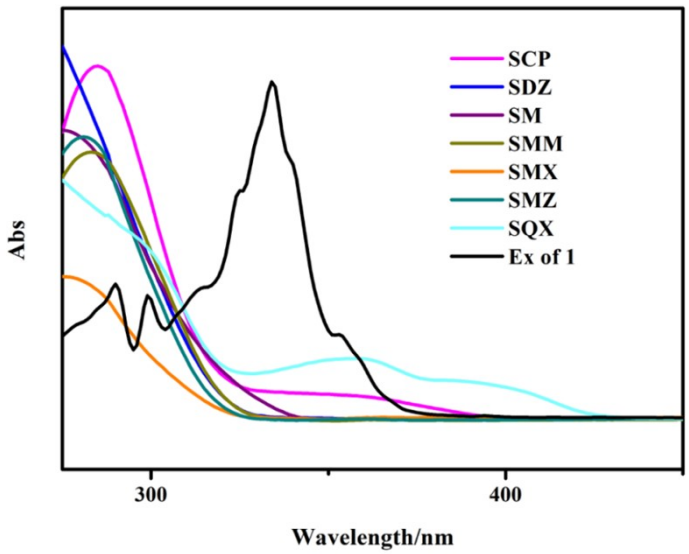

Figure S15. UV-vis absorption spectrum of sulfadiazine antibiotics and the excitation spectrum of complex **1**.

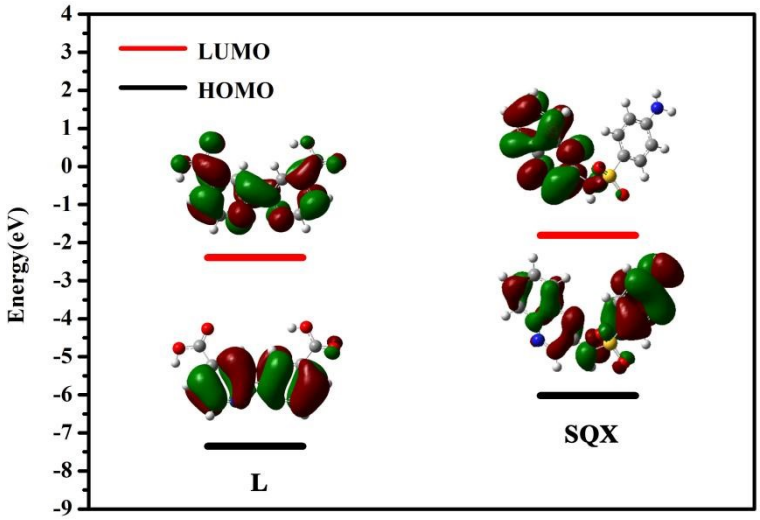

Figure S16. The HOMO and LUMO energies for SQX and L [B3LYP/6-31G(d)].

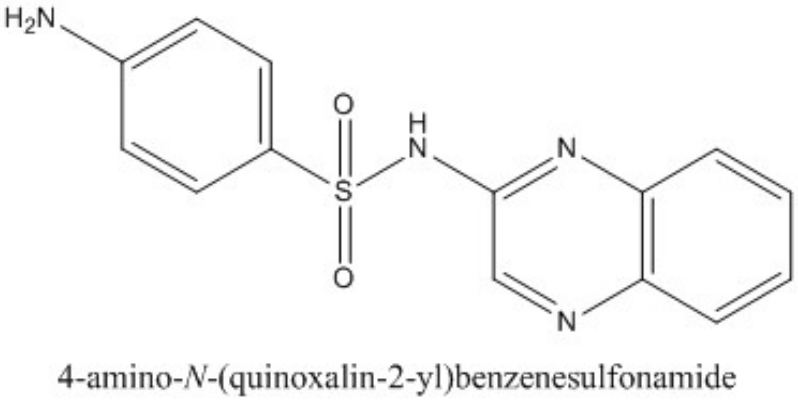

Figure S17. The structure of sulfaquinoxaline.

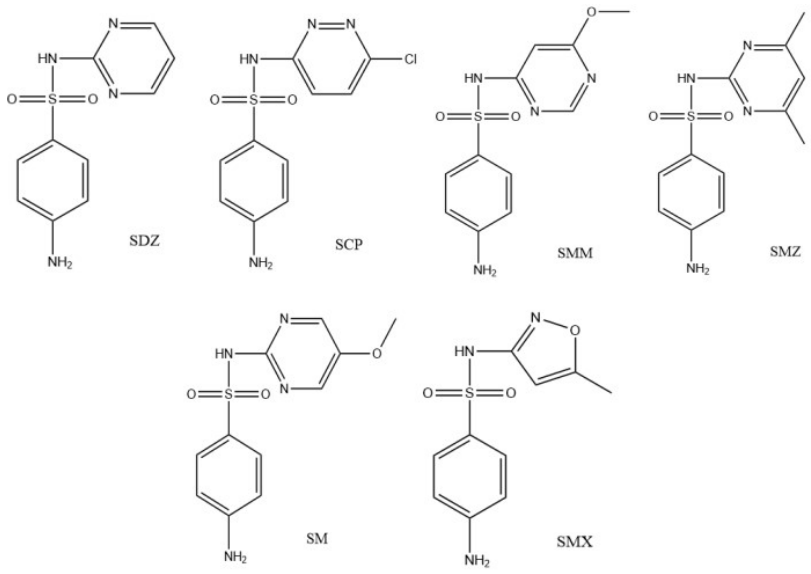

Figure S18. The structure of other sulfonamide drugs.

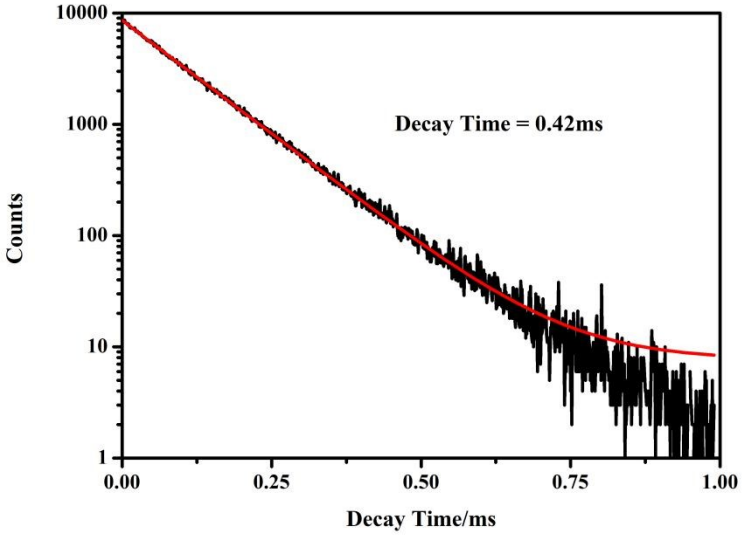

Figure S19. The fluorescence decay and fit curve for SQX@**1**.

References

[1] J. Qian, F. Quan, F. Zhao, C. Wu, Z. Wang, L. Zhou, Aconitic acid derived carbon dots: Conjugated interaction for the detection of folic acid and fluorescence targeted imaging of folate receptor overexpressed cancer cells, Sensors and Actuators B: Chemical, 262(2018) 444-51.

[2] K. Ren, X.-F. Guo, Y.-J. Tang, B.-H. Huang, H. Wang, Size-controlled synthesis of metal–organic frameworks and their performance as fluorescence sensors, Analyst, 145(2020) 7349-56.

[3] Y. Jiang, Y. Huang, X. Shi, Z. Lu, J. Ren, Z. Wang, et al., Eu-MOF and its mixed-matrix membranes as a fluorescent sensor for quantitative ratiometric pH and folic acid detection, and visible fingerprint identifying, Inorganic Chemistry Frontiers, 8(2021) 4924-32.

[4] X. Li, L. Chen, Fluorescence Probe Based on an Amino-Functionalized Fluorescent Magnetic Nanocomposite for Detection of Folic Acid in Serum, ACS Applied Materials & Interfaces, 8(2016) 31832-40.

[5] S. Yan, D. Deng, L. Zhang, Y. Lv, Fluorescence nano metal organic frameworks modulated by encapsulation for construction of versatile biosensor, Talanta, 201(2019) 96-103.

[6] K. F. Kayani; K. M. Omer, A red luminescent europium metal organic framework (Eu-MOF) integrated with a paper strip using smartphone visual detection for determination of folic acid in pharmaceutical formulations. New Journal of Chemistry 2022, 46 (17), 8152-8161.